Nucleic acid fragmentation on the millisecond timescale using a conventional X-ray rotating anode source: application to protein–DNA footprinting

Arnon Henn, Jacob Halfon, Itai Kela, Itzhak Orion[1] and Irit Sagi*

Department of Structural Biology and [1]Department of Particle Physics, The Weizmann Institute of Science, Rehovot 76100, Israel

Received as resubmission September 10, 2001; Accepted October 15, 2001

ABSTRACT

Nucleic acid fragmentation (footprinting) by ·OH radicals is used often as a tool to probe nucleic acid structure and nucleic acid–protein interactions. This method has proven valuable because it provides structural information with single base pair resolution. Recent developments in the field introduced the 'synchrotron X-ray footprinting' method, which uses a high-flux X-ray source to produce single base pair fragmentation of nucleic acid in tens of milliseconds. We developed a complementary method that utilizes X-rays generated from a conventional rotating anode machine in which nucleic acid footprints can be generated by X-ray exposures as short as 100–300 ms. Our theoretical and experimental studies indicate that efficient cleavage of nucleic acids by X-rays depends upon sample preparation, energy of the X-ray source and the beam intensity. In addition, using this experimental set up, we demonstrated the feasibility of conducting X-ray footprinting to produce protein–DNA protection portraits at subsecond timescales.

INTRODUCTION

Footprinting refers to assays in which either the binding of a ligand to a specific sequence of bases or the conformation of the nucleic acid inhibits nicking of the phosphodiester backbone of nucleic acid polymer by a reagent (1,2). Intimate interactions between proteins and nucleic acids are widely examined by footprinting methods. The prerequisite of such assays is the ability to produce and detect high-quality nucleic acid fragmentation around the protein-protected areas. Nucleic acid fragmentation can be achieved by using a variety of enzymatic and chemical reagents (3). This work is highly related to the development of chemical hydroxyl radical footprinting using Fenton chemistry (4–6) and peroxonitrous acid (7). Hydroxyl radicals engender breaks of the phosphodiester backbone in a non-specific sequence manner and, hence, can be utilized for footprinting assays. Using hydroxyl radical methods over enzymatic footprinting is advantageous because it provides great sensitivity to nucleic acid structures, such as sequence-dependent curvature (8) and RNA folding (9).

Nucleic acid cleavage by hydroxyl radical (·OH) is predominantly dependent upon the solvent accessibility of the phosphodiester backbone. Additionally, it is relatively insensitive to base sequence, and it is not important whether the nucleic acid is single or double stranded (10). ·OH can be generated by Fe-EDTA catalysis or by γ-rays, β particles, fast neutrons and X-ray radiation (11–13). The radiolysis of water by X-rays with energies from 100 eV up to the MeV range produces free electrons and ·OH according to the overall reaction illustrated in equation **1** (14)

$$H_2O \xrightarrow{h\nu} H_2O^+ + e^-_{dry} \xrightarrow{H_2O} H_3O^+ + \cdot OH + e^-_{eq} \qquad \mathbf{1}$$

The ·OH generated by this reaction can abstract a hydrogen from the C′4 carbon of the ribose sugar of DNA and RNA, leading to breakage of the phosphodiester backbone of the polymer (15). Controlled exposure of protein–nucleic acid complexes to X-rays has been used to detect specific interactions within such complexes (11,16). X-ray-mediated footprinting was shown to be an attractive method for time-resolved footprinting studies, because it can produce a high flux of ·OH that will fragment a nucleic acid backbone in millisecond timescales with base pair sensitivity. The recent development of synchrotron time-resolved X-ray footprinting demonstrated the utilization of this method to study the dynamic structural changes in RNA folding (17).

High radiation sources like synchrotron can produce a high enough photon flux to generate ·OH radicals with cutting power to the order of tenths of milliseconds (13). The most voluble parameter in applying an X-ray source to footprinting, besides speed, is the reproducibility that is achieved by radiation when compared with hand-mixing hydroxyl radical procedures (18). However, the limitation of a synchrotron radiation source lies in its accessibility to everyday users and its high cost of operation.

In this work, we report on the fragmentation of 140 bp DNA by X-rays generated from a conventional rotating anode machine. The presented footprinting method is rapid (100–300 ms), handy, simple to operate and reproducible. The X-ray source was optimized for nucleic acid footprinting by monitoring the radiation intensity and the X-ray energy. The optimization of the X-ray source was also studied by Monte Carlo

*To whom correspondence should be addressed. Tel: +972 8 9342130; Fax: 972 8 9342130; Email: irit.sagi@weizmann.ac.il

theoretical simulation. In addition, we report the sample preparation procedure required to achieve a lower footprinting timescale. The application of these factors to the data acquisition procedure enabled us to perform the ·OH radical footprinting of DNA in timescales suitable for studying the structural kinetics of RNA folding (19) and protein–nucleic acid interactions (20). Finally, we demonstrated the application of this method to protein–DNA footprinting by mapping the protection patterns of integration host factor (IHF) from *Escherichia coli* on its target DNA substrate.

MATERIALS AND METHODS

DNA cloning and plasmid purification

A random fragment from *E.coli* isolated chromosomal DNA, restricted with *Bam*HI and *Eco*RI restriction enzyme, was cloned into pre-digested pTZ18R (Amersham Pharmacia Biotech) with the same enzymes. After transforming *E.coli* XL-1 Blue strain (Stratagene), the plasmid was amplified and purified using a concert nucleic acid purification system kit (Gibco BRL). A DNA fragment was cut by enzymatic restriction to produce a fragment of 140 bp; it was purified with a Millipore DNA purification kit from 1% agarose gel.

Preparation and end labeling of DNA molecules

DNA was end labeled with Klenow fragment (Roche Molecular Biochemicals) with [α-^{32}P]ATP using standard protocol. The labeled DNA was loaded into 8% PAGE/TBE × 1.0 and the DNA fragment was excised from the gel. The DNA was extracted from the gel by electroelution using the Schleicher and Schuell BIOTRAP system. DNA was precipitated and resuspended in 10 mM cacodylate buffer, pH 7.5.

Chemical footprinting

Fe(II)-EDTA cleavage reactions were performed by the method of Tullius and Dombroski (21) with slight modification (K.J.Hampel, personal communication). Cleavage reaction components, 1 µl of 0.2% H_2O_2, 1 µl of 60 mM sodium ascorbate and 1 µl Fe(II)-EDTA [60 mM $Fe(NH4)_2$-$(SO_4)_2$ and 50 mM Na_2-EDTA pH 8, mixed prior to chemical reaction] were added sequentially to the inside wall of the reaction tubes. Rapid mixing was then applied by tapping on the outside part of the Eppendorf tube. Reactions were allowed to proceed for 2 s and then quenched with 90 µl of 100% ethanol, 0.3 M sodium acetate pH 5.2, 0.4 µg tRNA, precipitated in –20°C and resuspended in loading buffer.

X-ray footprinting

DNA footprinting was performed in siliconized microtubes in volumes of 10 µl, 60 000 c.p.m. specific activity and were incubated on ice before exposure to X-rays. Each sample was placed and exposed to X-rays as described in Scheme 1. The X-ray shutter was open for the indicated time windows. Immediately after exposure to X-rays, the samples were put on ice and combined with an equal volume of loading buffer: 90% formamide, 0.5× TBE buffer, 1 mM EDTA and 0.05 (w/v) xylene cyanole. Samples were kept at –80°C for further analysis.

Protein–DNA footprinting

Purified IHF protein and its DNA substrate were kindly provided by Dr Michael Brenowitz and Gurie Dhavan. IHF was stored in Tris–HCl pH 7.5, 200 mM NaCl, 1 mM EDTA and 5% glycerol. The target DNA substrate of IHF (see Fig. 5A) was prepared by PCR amplification of a plasmid carrying an IHF consensus sequence (22). The resulting PCR product of 164 bp was pre-phosphorylated in one of its primers with cold ATP before the PCR reaction. The second phosphorylation was performed after the PCR with [γ-^{32}P]ATP, using standard T4 polynucleotide kinase (NEB). DNA was electroeluted as describe above. Footprinting reactions were performed in 20 mM cacodylate buffer at pH 7.5, 50 mM KCl, 1 mM $MgCl_2$, at room temperature after 10 min. The reaction was quenched by ethanol precipitation, resuspended in loading buffer and analyzed by gel electrophoresis.

Gel electrophoresis

Samples were applied to a pre-warm 10% denaturing polyacrylamide sequencing gel. Electrophoresis was performed at 50°C buffered with 1.0× TBE. After completing the run, the gels were fixed with 10% acetic acid and 10% methanol for 20 min, followed by incubation of the gel in 10% glycerol for 20 min. Autoradiographs of the dried gels were analyzed by densitometry using Molecular Dynamics (MD) PhosphoImager Storm 820.

Data analysis of footprinting experiments

Data were analyzed with ImageQuantNT software (MD). Quantification of fraction uncut was calculated according the following formula:

$$F = \frac{OD_{n,\,cut}}{OD_{uncut}} \qquad \mathbf{2}$$

Where F equals the fraction uncut, $OD_{n,\,cut}$ is the measured intensity of the nth band, and OD_{uncut} is the unexposed sample measured intensity. The data were fitted to a semi-logarithmic plot to exponential decay 1st order: $Y = y_0 + Ae^{-x/t}$. Each data point is an average of two independently performed experiments.

Design of the X-ray source

Scheme 1 shows a schematic representation of the hardware modifications that were applied to a conventional rotating anode machine (X-ray generator, model RTP 500; Rigaku, Japan). The inserted devices are made of brass. The costume design of this apparatus has the advantage of directly irradiating the sample with the X-ray beam without any divergence.

Manual shutter set up

In the first set of experiments, we used the manual mechanical shutter (Scheme 1, part MMS) of the X-ray generator for control of the exposure time at second timescales. In these experiments, the sample was placed at the bottom of the Eppendorf tube. The X-ray beam traveled 3.6 cm in the air from the MMS to the Eppendorf tube. The test tube holder was positioned at the center of the X-ray beam [Scheme 1, EH (Eppendorf holder) part A].

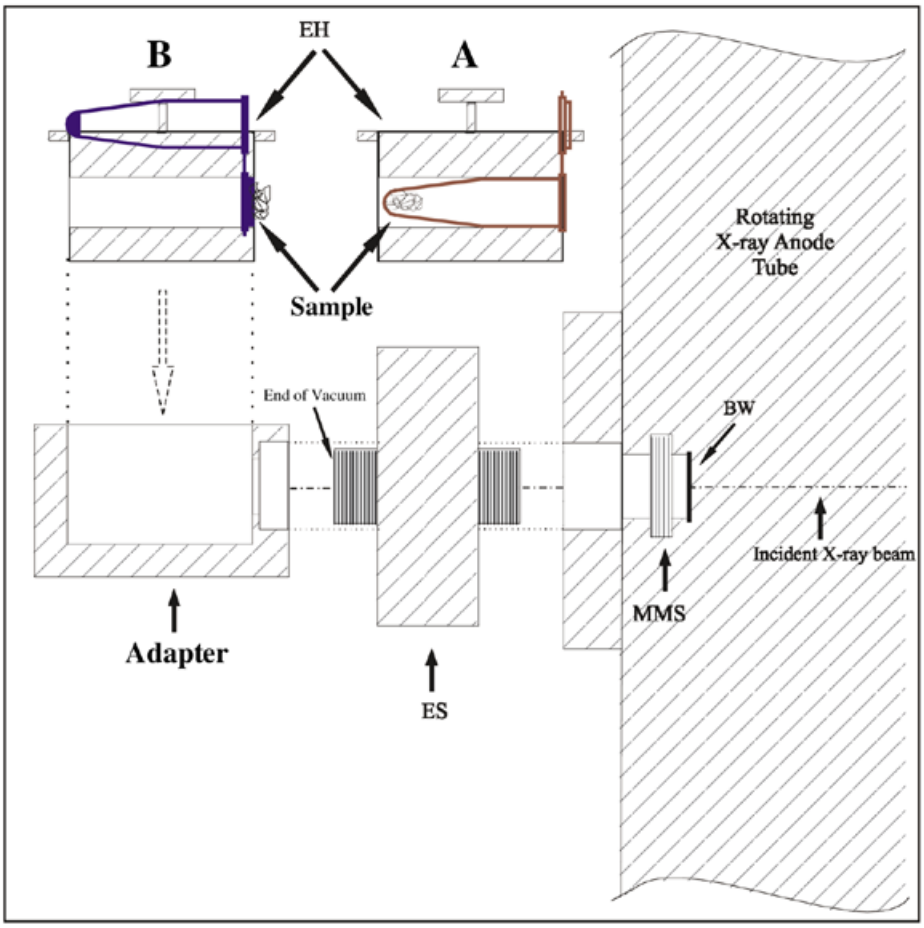

Scheme 1. Schematic representation of the rotating anode X-ray set up. The incident X-ray beam is controlled by the MMS switch (part MMS) and the intensity is maintained by the X-ray generator control board. In the first set up, the Eppendorf adapter is connected right after the MMS. The sample in the Eppendorf is inserted into the adapter by using the EH as in A. The MMS can be controlled for a 1 s or more timescale only. In the second set up for time-resolved footprinting studies, an ES was inserted before the adapter. The X-ray beam is kept in a vacuum until it irradiates the sample. To minimize the path of the X-ray beam outside the vacuum, the sample is positioned inside the cap of the Eppendorf, which is held by a modified EH as in B. After the sample is positioned, the MMS is switched on, and the ES is controlled by a remote box for millisecond exposure.

Electronic shutter set up

We installed an electronic shutter (Scheme 1, part ES; Vincent Associates, Rochester, NY) between the MMS and Adapter for the EH (Scheme 1) to conduct dose-response experiments in millisecond timescales. The shutter set up was kept in a vacuum until the X-rays exited. To further minimize the distance that the X-ray traveled in air between the DNA sample and the source, we placed the DNA sample in the Eppendorf tube cap. The ES was controlled through a cable by a remote control box (commercially available; Vincent Associates, Rochester, NY). The ES was rigorously tested for X-ray resistance. Once the sample was inserted into position, the X-ray machine shutter was opened, immediately followed by the release of the ES at the selected time frame. The irradiated DNA solution was inserted back into the tube by closing the Eppendorf cap, followed by a short centrifugation.

Monte Carlo theoretical simulations of the photon absorption

The last developments in the EGS4 code system (23) for low-energy scattering and polarization established the code system as one of the best tools for synchrotron-based X-ray simulations. The modular structure of the low-scattering photon transport routines, developed by the KEK EGS group (24,25), enabled us to prepare compound cross sections with form factors and scattering functions as H_2O, air, DNA (as a polymer of $C_5O_5H_7$-P) and polypropylene. The EGS4 system was used to simulate the deposited energy in the footprinting samples for different photon sources. The first user-code was developed to include the National Synchrotron Light Source (NSLS) beam line X9-. A spectrum shape was calculated by information found on the web (http://www-cxro.lbl.gov/optical_constants/bend2.html). Conditions used for the calculation were 92% linear polarization ratio, introducing the DNA sample inside the conical end of a polypropylene 'Eppendorf' tube (1.5 ml), sealed by a 1 mm cover made of the same material. The absorbed energies per incident flounce in the cover and in the sample were scored to find the efficiency of the NSLS photon source for footprinting.

Another group of user-codes was written for the X-ray generator footprinting irradiation system, which included the filtration (Be and air), the source energy due to the anode material

and the sample inside the opened polypropylene cylinder (as shown in Fig. 1). The same outputs were applied in the X-ray generator simulations as in the NSLS simulation, with 10^7 histories for each.

RESULTS

The fragmentation of nucleic acid has been shown to be dependent upon the effective concentration of free radicals, which are generated from water radiolysis (26). In the case of X-ray footprinting, the concentration of free radicals in solution is controlled by monitoring the X-ray exposure ('dose') received by the DNA/RNA sample. The experimentally determined dose-response curve provides the required X-ray exposure time in which each DNA/RNA molecule is cleaved only once. X-ray exposures resulting in 10–30% of the nucleic acid cleavage implement this requirement. We have optimized the sample preparation procedure and the buffer system used in these experiments by conducting dose-response experiments for the different reaction conditions.

Sample preparation

We minimized the factors that contributed to ·OH radical scavenging to increase the effective concentration of the free radicals in solution. The purification of labeled DNA is usually conducted by extraction from the polyacrylamide gel matrix. This procedure introduces remnants of polyacrylamide in the extracted DNA/RNA solution. Therefore, we purified the DNA from the gel matrix by electroelution. This method remarkably lowered the required exposure time of the nucleic acid sample to the X-ray beam to achieve 10–30% of nucleic acid cleavage. In addition, we tested three buffer systems (pH 7.5, 10 mM): Tris–HCl, HEPES–Na and cacodylic–Na. The best results were obtained with the cacodylate buffer. This buffer system is used often in X-ray footprinting procedures (13,18). Overall, these results show that sample composition and purification play a key role in the X-ray footprinting assay generated by the rotation anode machine. Apparently, the sample preparation procedure is less effective in synchrotron X-ray footprinting because the high flux of X-ray photons generates a high concentration of ·OH radicals, which compensate for the radical scavenging by the solution components.

Rotating anode parameters

The photon flux intensity and the energy of the rotating anode X-ray source must be optimized to achieve maximum yield of nucleic acid fragmentation.

The X-ray beam parameters were optimized using both theoretical and experimental studies. The photon flux generated by the X-ray beam can be calculated for a given operation power and material target. The photon spectral flux for common diagnostic X-ray generators was calculated and summarized in a catalogue (27) for a variety of anode materials and tube voltages. The referenced flux value per Amp was multiplied with our rotating anode current to calculate the photon flux exiting the source. The flux per Amp value of 1.91×10^6 ph mA^{-1} s^{-1} mm^{-2} for the molibdium (Mo) target, at 50 kV tube voltage, was selected from the catalogue as a reference value without adding filtration, because the filtration was included in the EGS4 Monte Carlo user-code simulation. The source photon flux for a Mo rotating-anode (300 mA) is, therefore, 5.7×10^8 ph s^{-1} mm^{-2} at 17.48 keV. The photon flux of other low Z-number target materials [such as copper (Cu), chromium (Cr), nickel (Ni), iron (Fe) anodes] at the Kα emission lines can be compared due to the Mo florescence yields ratios. These results show that the photon flux generated from rotating anode is one order of magnitude lower than the photon flux used in synchrotron footprinting experiments (200 mA ring current generates 5×10^9 ph s^{-1}) (17).

Table 1. Rotating anode parameters

Target	Energy (KeV)	Calculated photon flux (ph s^{-1} mm^{-2})	Calculated energy fraction absorbed in the sample (%)	% Fraction cleaved 1 s X-ray exposure[a]
Silver (Ag)	22.162	6.2×10^8	9.36	4
Molibdium (Mo)	17.478	5.7×10^8	17.84	14
Copper (Cu)	8.047	3.3×10^8	81.13	21

The energy parameters and the theoretical values of photon flux exerted by the X-ray generator and the fraction of X-ray absorbed by the sample due to the shape of the sample and the composition of the reaction. (See Materials and Methods for detailed discussion on the calculation for theoretical and experimental data.) Calculations and experiments were performed for 15 kW conditions (300 mAmps and 50 KeV).
[a]An average of two independent samples.

To calibrate the specific beam energy with the shortest timescales required for effective nucleic footprinting, we tested three different target elements used as anodes. The effect of the X-ray energy source on the amount of DNA cut was examined at a given time by conducting dose-response experiments. In this experiment we used silver (Ag), Mo and Cu target anodes, which represent a relatively wide range of energy: Ag, λ = 0.56 Å (25.5 KeV); Mo, λ = 0.71 Å (19.9 KeV), Cu λ = 1.54 Å (8.97 KeV).

The results of these experiments, as well the calculated values of the photon flux generated from each anode and the percent energy fraction absorbed in the sample, are summarized in Table 1. The Monte Carlo theoretical simulation was conducted following reported procedures (see Materials and Methods).

Table 1 clearly shows that the Cu anode achieved the most efficient DNA fragmentation, at the given X-ray generator set up, because most of the generated energy is deposited in the sample. Furthermore, our results show that the main factor of efficient DNA cleavage is the amount of energy absorbed in the sample, which is correlated by the specific energy of the source (Table 1). To further examine the effect of beam energy on DNA fragmentation, we initiated Monte Carlo calculations. In the case of X-ray generators with different anode metals, the absorbed energy resulting from the Monte Carlo simulations was introduced to optimize the rotating anode selection due to the maximum sample radiation absorption. The fluorescence yield of each material was multiplied on the flux to compare the absolute sample absorptions (see also in Table 1). Figure 1 shows the simulation results of sample absorption efficiency versus the anode material Z-number. These results show that the energy at KeV between 7 and 9.5 contributes the most to the fragmentation of DNA in an aqueous solution. This range of energy is consistent with the energy of a Cu rotating anode (9 KeV). Therefore, the Cu rotating anode was found to be the

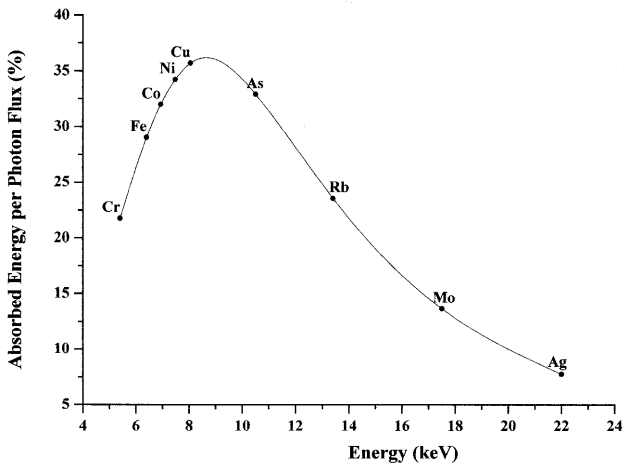

Figure 1. Monte Carlo simulations of the absorbed energy in the DNA sample by different rotating anode target elements. Theoretical simulations of the absorbed energy per photon flux in the nucleic acid sample for several rotating anode target source materials. The peak at 9 KeV indicates that the Cu anode is near the optimal choice for performing footprinting with a conventional X-ray rotating anode system. The various data points were calculated as described in Materials and Methods.

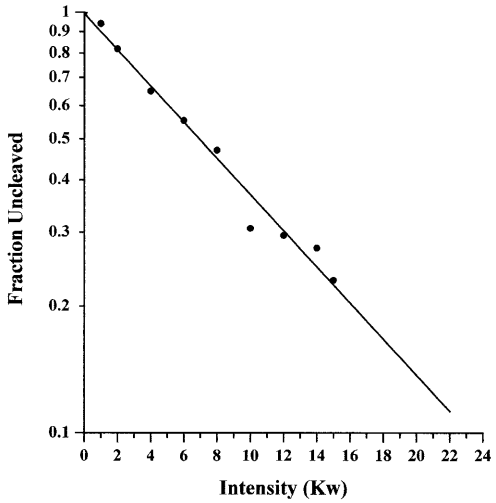

Figure 2. X-ray beam intensity effect on DNA fragmentation. Dose-response curve of beam intensities versus fraction of uncleaved DNA. DNA samples of ~60 000 c.p.m. were exposed to the X-ray beam with Cu target source for 3 s at different beam intensities (Kw = KeV·mAmps). DNA samples were analyzed by urea/PAGE electrophoresis. The amount of cleaved DNA was quantified as described in Materials and Methods. The data sets represent two independent determinations. The fragmentation of DNA shows a linear relationship to the intensity of the X-ray generator. The linear fit was extrapolated to higher intensity to show the effect of the beam flux (intensity) on the fragmentation of DNA ($R^2 = 0.98$).

most appropriate material for use with X-ray generator-based footprinting.

X-ray beam intensity

The beam intensity parameter and its relation to percent DNA cut was examined. Figure 2 shows the relationship between the intensity of the X-ray beam and the fraction of uncut DNA after exposure to X-rays. The samples were exposed to the X-ray beam for a constant time of 3 s. These results show that the intensity of the source has a linear relationship with the fraction of DNA cut. Theoretical extrapolation of the linear line indicates that higher beam intensities resulted in increased percent of DNA fragmentation in less time. Thus, a combination of the appropriate source energy with the highest intensity that can be achieved by the X-ray generator will contribute to maximum yield of DNA fragmentation in minimal timescales.

Resolving DNA at base pair resolution

Following nucleic acid fragmentation at base pair resolution requires the nucleic acid fragmentation method to show no discrepancy in cutting preferences. In addition, the electrophotogram of the nucleic acid fragments should be able to resolve long DNA/RNA molecules with a high resolution of band separation. A hydroxyl radical had been shown to produce such a pattern of cleavage from both chemical and X-ray sources (13,28).

Figure 3 shows the portrait of 140 bp DNA fragment after exposure to the rotating anode X-ray beam for 1–4 s. The results were comparable with the DNA cleavage patterns obtained by Fe(II)-EDTA protocols (18). The X-ray rotating anode footprinting in Figure 3 shows exceptionally uniform and reproducible cleavage patterns (see insert). The integrated band intensity analysis shows a highly homogeneous pattern throughout a long region of separated gel bands (29). To better resolve the DNA fragments during electrophoresis, we used wedge gel spacers, which increase the length of separation of nucleic acid as well as the uniformity of the bands. With this arrangement, we can resolve up to 120 bp of a DNA molecule with sufficient quality to perform quantitative footprinting analysis. It is important to note that the results presented in Figure 3 are highly consistent and reproducible. It may be that this is due to the stability of the rotating anode X-ray source in terms of constant photon flux and intensity.

Time resolution of DNA fragmentation

The introduction of time-resolved synchrotron X-ray footprinting opened the possibility of investigating a wide spectrum of protein–nucleic acid interactions in short timescales (30). To further improve the time resolution of DNA fragmentation using our apparatus, we installed an X-ray resistant ES to control the exposure of samples to milliseconds. The ES is aligned with the X-ray beam, and the X-ray can pass through only if both the manual and ES are opened (Scheme 1). Furthermore, to minimize the path traveled by the X-ray beam in air, we used the Eppendorf cover cap to hold the sample as close as possible to the end of the vacuum line facing the exit of X-rays (Scheme 1, Eppendorf position). With this improved arrangement, we were able to lower the time required to achieve 10–30% DNA cleavage of the given DNA fragment to the millisecond time regime.

Figure 4 shows the dose-response results of the 140 bp DNA fragment. The percent DNA cut was measured after exposure to the X-ray source in millisecond timescales. The dose-response densitometry analysis shows that 10% cleavage occurs in 300 ms (Cu 60 KeV, 300 mA). Close examination of the signal-to-noise ratio of individual band intensities allows the performance of quantitative footprinting data analysis at timescales as low as 100 ms (13). Figure 4 (insert) shows the densitometry scans through the 140 bp DNA fragment in

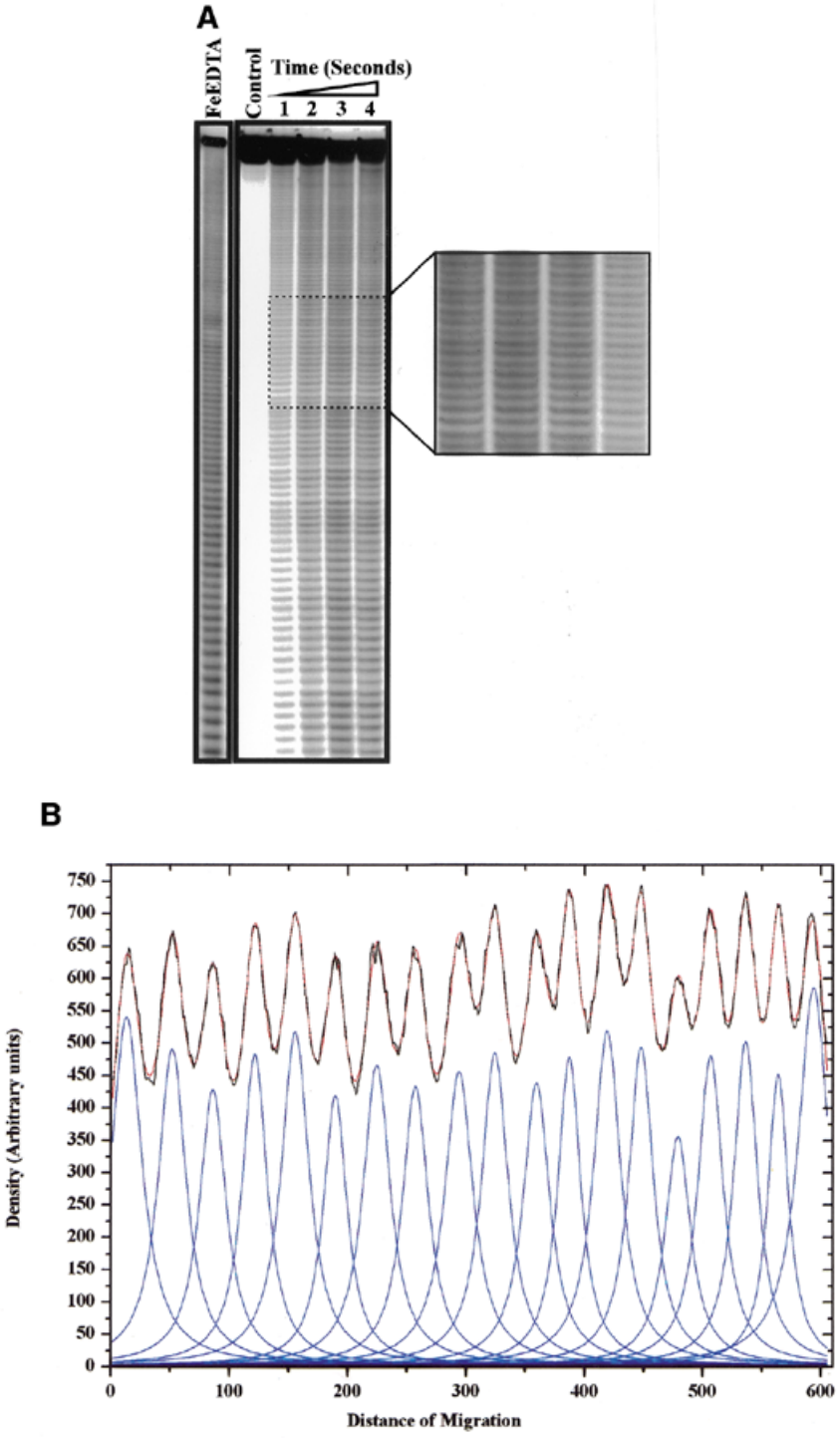

Figure 3. DNA fragmentation by rotating X-ray anode in base pair resolution. (**A**) A base pair resolution portrait of 140 bp DNA fragment after exposure to the X-ray beam. The digital image was obtained by phosphor storage imaging of a 12% urea/PAGE wedge-spaced gel of the reaction products resulting from a 1–4 s exposure to the X-ray beam of a 140 bp DNA ^{32}P-labeled restriction fragment. The lane designated FeEDTA was treated with the Fenton reaction on the same DNA preparation, but was analyzed on a separate gel using the same conditions as describe above. The insert is an enlargement of the indicated area. (**B**) Peak fitting demonstration of the band intensities resulted from the cleavage pattern of the DNA. The data analysis was performed as described by Pastor *et al.* (29). The red graph represents raw data obtained from the program ImageQuant 5.0 (MD) and the blue graph presents the data after performing peak fitting.

various exposure times to the X-ray beam. The integrated band intensities at 100 ms show a 3-fold increase in band intensity over the background and 10-fold increase at 1 s. These results demonstrate the feasibility of using a conventional X-ray source for performing time-resolved, quantitative footprinting studies of nucleic acids at hundredths milliseconds time range.

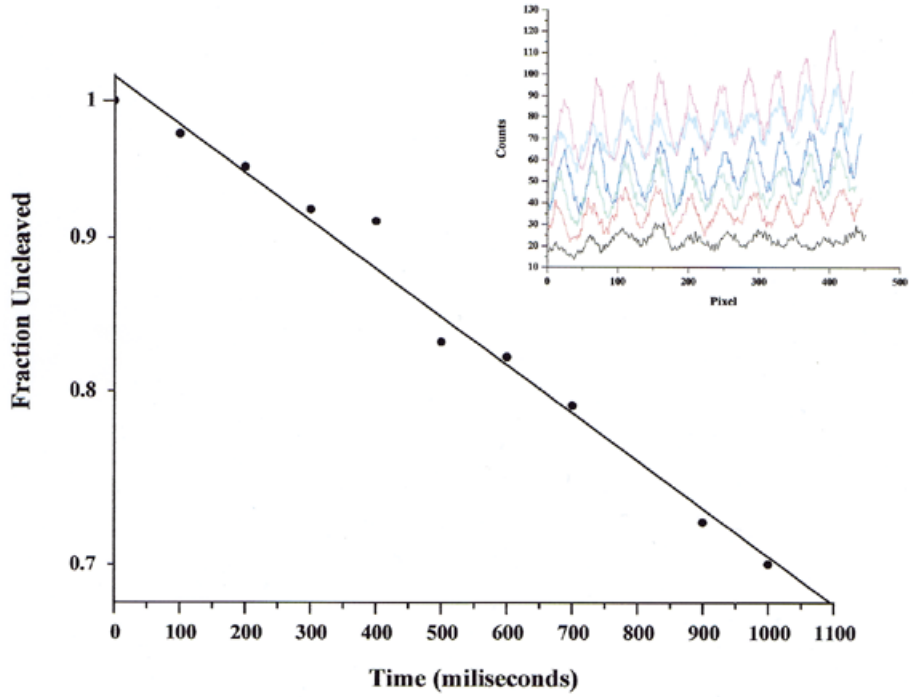

Figure 4. DNA fragmentation at milliseconds timescale. Dose-response curves relating the amount of uncleaved DNA to the time of sample exposure to the X-ray source, controlled by milliseconds shutter. Quantification of the fraction uncleaved was calculated as described in the Materials and Methods. The data set is an average of two independent determinations. The top right insert represents various densitometry scans through a region of 10 bases in the middle region of the gel. The scans from bottom to top are of 0 (background) (black), 100 (red), 300 (green), 500 (blue), 700 (cyan) and 1000 (pink) ms. The data show that quantitative data analysis can be performed between 100 and 300 ms (3-fold or more signal-to-noise ratio).

Protein–DNA footprinting

The application of a conventional X-ray source device to perform protein–DNA footprinting experiments was tested on IHF protein bound to its target DNA sequence. This complex was characterized by both biochemical and structural studies (22,31). IHF binds tightly to three sites along a 34 bp region (Fig. 5A). These sites produce three protection regions on the DNA target. Figure 5B shows IHF–DNA footprinting by both Fe(II)-EDTA and X-ray methods. The protein binding sites on the target DNA are marked as AI, AII, AIII, according to their corresponding sequences. These binding sites were analyzed by both Fe(II)-EDTA and our X-ray procedures. The Fe(II)-EDTA reaction was allowed to proceed for 2 s; the X-ray experiments were conducted by irradiating the samples with single exposure of 500 ms. Figure 5B lanes 1 and 4 show that the three designated IHF binding sites can be clearly identified by Fe(II)-EDTA and X-ray footprinting. Furthermore, these results are in good agreement with recent studies by Dhavan *et al.*, which report the footprinting pattern of the same IHF–DNA complex using the synchrotron X-ray footprinting procedure (G.M.Dhavan, D.M.Crothers, M.R.Chance and M.Brenowitz, submmited for publication).

DISCUSSION

In this paper, we have described X-ray footprinting procedures using a conventional X-ray generator. These procedures provide a new application for time-resolved X-ray footprinting of nucleic acid and protein–nucleic acid complexes conducted in local laboratories. Free ·OH radicals mediated by water radiolysis using a synchrotron X-ray source have proven to be a valuable probe of nucleic acid structure and nucleic acid–protein interactions (30). This method provides structural resolution to a single base pair. In addition, quantitative structural information can be obtained in a time-resolved manner within milliseconds timescales (13). However, using a synchrotron X-ray source for footprinting is expensive and immovable; the accessibility to beam lines is limited as well. Following the pioneering work of synchrotron X-ray footprinting (13), we developed a complementary method using conventional X-ray source.

Interactions of X-rays with matter involve the processes of photoelectric effect, coherent scattering and incoherent scattering. The contribution of each effect depends on the photon energy, and it is available for all elements and for most of the common use molecules (32). The contribution of each effect is related to the particle characteristics or the photon energy. In the case of X-rays in the KeV range, the absorption of a photon in water promotes an electron to an unbound state, with kinetic energy equal to the incident photon energy minus the ionization energy (17). The deposited electrons are responsible for the water ionization and the production of free ·OH radicals (equation **1**). The calculations of the effective concentration of generated free ·OH radicals in water also apply to diluted aqueous solutions where the photon interacts primarily with the water (33).

The dose absorption of an X-ray photon in water is highly dependent on the source spectrum. Therefore, the characteristics

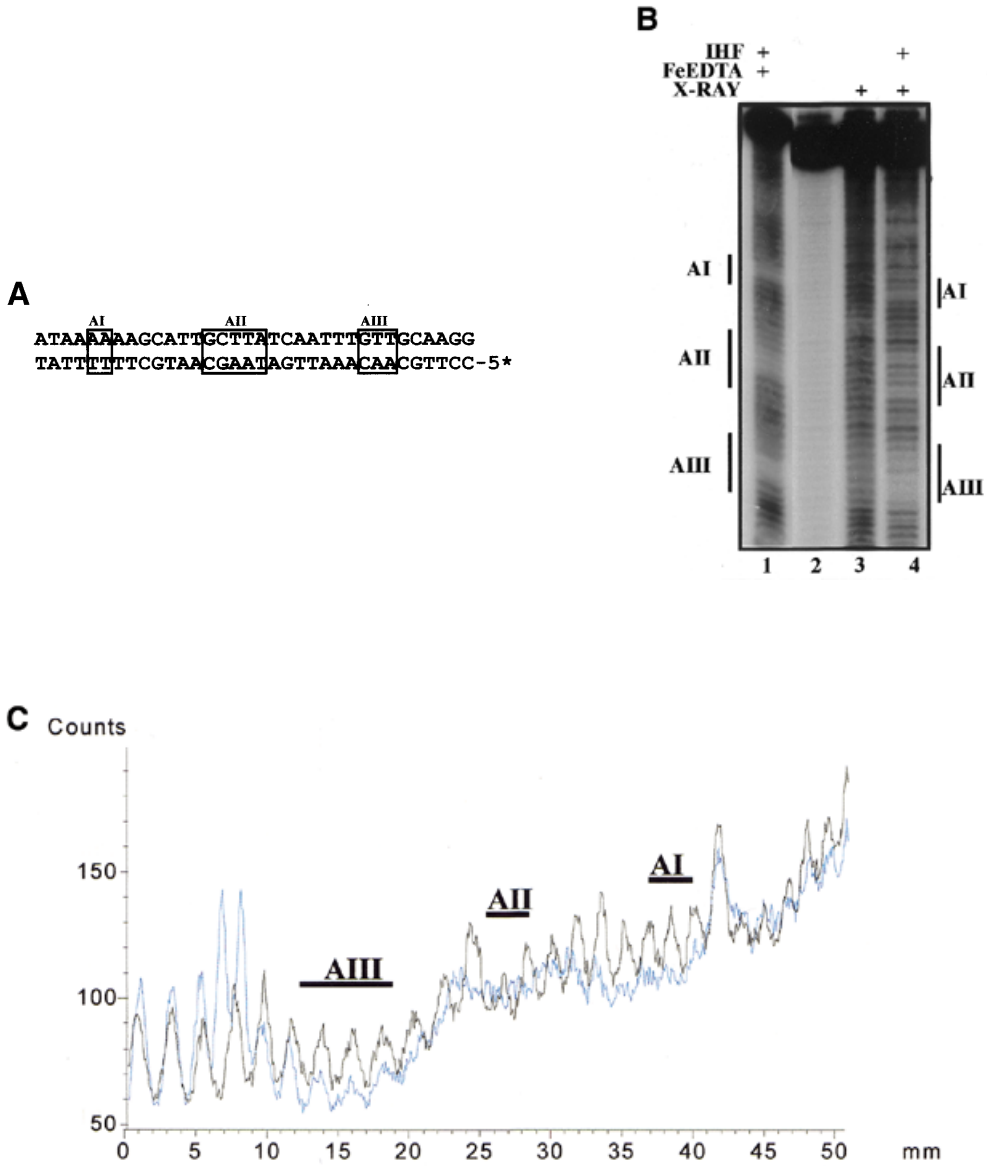

Figure 5. Footprinting of IHF–DNA complex by conventional rotating X-ray anode. (**A**) The IHF binding DNA sequence is shown in detail. The three binding sites of IHF on its target DNA region of 34 bp are marked in black boxes AI, AII and AIII. The interaction of IHF with its substrate DNA produces three protection regions. The 5′ end designated with an asterisk marks the position of ^{32}P-labeling. (**B**) Ten percent sequencing gel of 165 bp DNA ^{32}P-labeled, containing a 34 bp region of IHF binding sequence. IHF (50 nM) was incubated with its target DNA in 10 µl reaction volume at room temperature for 10 min. The sample was exposed to Fe(II)-EDTA cleavage (lane 1) or to X-ray beam for 1 s (lane 4). Lane 2 is the control DNA and lane 3 is free DNA exposed to X-ray. The three binding sites resulted from the tight binding of IHF with the 34 bp DNA region are marked AI, AII and AIII. All three sites are identified in both lanes 1 and 2. (**C**) Densitometry profiles of (B), lanes 3 and 4 (black and blue, respectively) showing a decrease in peak intensities upon binding of IHF on the DNA (B, lane 4).

of the X-ray generator were investigated to develop an available local laboratory source. We compared the total absorbed dose and the energy deposit spectra in a nucleic acid sample from a synchrotron X-ray source and from different anode material of an X-ray generator source. The calculated photon flux incident on a sample after passing through the beam line optics and air path of 40 cm is 2×10^{11} photons mm^{-2} s^{-1} (beam line operated at 2.54 GeV, 250 mA) with peak energy at 10 KeV. The calculated photon flux incident on the sample in the X-ray generator set up presented in Scheme 1 (50 kV, 250 mA) is in the order of 3.3×10^{8} photons mm^{-2} s^{-1} for Cu rotating anode at 9 KeV.

Comparisons of the normalized source spectrum and deposited spectrum on the nucleic acid sample are presented for the synchrotron beam and for various X-ray anodes in Figure 6. The results show that the Cu rotating anode energy is highly consistent with the peak energy absorbed by the sample in the synchrotron source. However, in contrast to the wide range of energies applied to the sample by the synchrotron X-ray beam, the Cu anode spectrum provides a single or very narrow energy

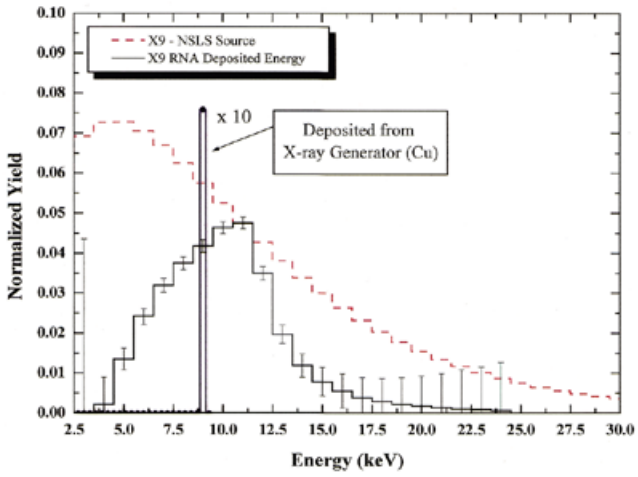

Figure 6. The normalized photon flux spectrum at the X-9 NSLS beam line compared with the normalized absorbed energy distribution on a nucleic acid sample in aqueous solution. The peak energy on the sample falls between 11–12 KeV, in agreement with the results shown in Tullius *et al.* (28). The error bars represent the simulation results standard deviation. The energy peak deposited from the X-ray generator with Cu anode source (dot line) falls very close to the peak of the energy deposited from the X-9 NSLS.

range. Overall, these results show that the energy of the absorbed photon, above a given value of photon flux, may be considered as a limiting factor for effective DNA cleavage by X-rays in dilute solutions. Therefore, the material of the target in the rotating anode generator should be carefully selected to obtain effective nucleic acid cleavage in short timescales. Nevertheless, up to 81% of the energy provided by the Cu anode is absorbed in the DNA solution (Table 1), which improves the probability of DNA cleavage by the free ·OH radicals.

The adjustment of sample composition and buffer conditions in the described footprinting is very important because of the relatively low photon flux generated from conventional X-ray generators. Although the sample composition used for ·OH radical and specifically for X-ray footprinting was widely discussed (5,18,30), it is important to note that the effect of radical scavenging is enhanced more using a conventional X-ray generator, due to the low photon flux. Therefore, we applied the reported procedures for sample preparations and buffer composition prior to exposure to X-rays.

Recent studies by Hample and Burke (18) introduced the application of time-resolved hydroxyl radical footprinting using high doses of Fe(II)-EDTA. Some advantages of this procedure are that inexpensive and commonly available reagents are utilized, and timescales as low as 2 s can be reached. However, the authors claim that the variation in the extent of nucleic acid cleavage caused by hand-mixing problems increases the experimental error and makes it difficult to quantify the data. In contrast, the X-ray footprinting portraits generated by the rotating anode source are extremely reproducible. The consistency among the various samples is due to the stability of the optimized X-ray source that operates in a constant photon flux and intensity.

X-ray footprinting using a conventional X-ray machine provides improved time resolution with high-structural resolution and general applicability to the study of protein–nucleic acid interactions, when compared with other time-resolved bench-top footprinting methods. The footprint of the IHF–DNA complex shown in Figure 5 demonstrates the feasibility of producing protein–DNA footprints with a conventional X-ray source. The decrease in time resolution between DNA fragmentation and protein–DNA footprint is due to the presence of radical scavengers (e.g. glycerol) in the protein buffer solution. Improvement in footprinting timescales can be achieved by lowering the amount of potential radical scavenger components in the buffer composition. Nevertheless, obtaining highly reproducible protein–DNA footprinting patterns in sub-second timescales has an advantage over other alternative methods presented to date in the aspects of both time resolution and accuracy.

In this work, we propose a rapid and handy X-ray-based footprinting method to be used in local laboratories for various applications, including RNA folding, protein–nucleic acid footprinting (34), and the mass screening of protein–nucleic acid complexes merged from large-scale projects such as the Human Genome Project. It is important to note that this method cannot approach the time resolution obtained by synchrotron footprinting (30). However, it may provide an excellent alternative for relatively slow dynamic processes of both nucleic acid and protein–nucleic acid interactions.

ACKNOWLEDGEMENTS

We thank Drs Michael Brenowitz, Mark Chance and Gauri Dhavan for helpful discussions and guidance and for providing us with purified IHF protein and its DNA substrate. We also thank Ken Hampel for his help with Fenton reaction protocol. This work was supported by the Minerva foundation. I.S. is incumbent of the Robert Edward and Roselyn Rich Manson Career Development Chair.

REFERENCES

1. Tullius,T.D. (1989) Physical studies of protein-DNA complexes by footprinting. *Annu. Rev. Biophys. Biophys. Chem.*, **18**, 213–237.
2. Brenowitz,M., Senear,D.F., Shea,M.A. and Ackers,G.K. (1986) Quantitative DNase footprint titration: a method for studying protein-DNA interactions. *Methods Enzymol.*, **130**, 132–181.
3. Galas,D.J. and Schmitz,A. (1978) DNAse footprinting: a simple method for the detection of protein-DNA binding specificity. *Nucleic Acids Res.*, **5**, 3157–3170.
4. Tullius,T.D. and Dombroski,B.A. (1986) Hydroxyl radical 'footprinting': high-resolution information about DNA-protein contacts and application to lambda repressor and Cro protein. *Proc. Natl Acad. Sci. USA*, **83**, 5469–5473.
5. Tullius,T.D., Dombroski,B.A., Churchill,M.E. and Kam,L. (1987) Hydroxyl radical footprinting: a high-resolution method for mapping protein-DNA contacts. *Methods Enzymol.*, **155**, 537–558.
6. Strahs,D. and Brenowitz,M. (1994) DNA conformational changes associated with the cooperative binding of cI-repressor of bacteriophage lambda to OR. *J. Mol. Biol.*, **244**, 494–510.
7. King,P.A., Jamison,E., Strahs,D., Anderson,V.E. and Brenowitz,M. (1993) 'Footprinting' proteins on DNA with peroxonitrous acid. *Nucleic Acids Res.*, **21**, 2473–2478.
8. Burkhoff,A.M. and Tullius,T.D. (1987) The unusual conformation adopted by the adenine tracts in kinetoplast DNA. *Cell*, **48**, 935–943.
9. Latham,J.A. and Cech,T.R. (1989) Defining the inside and outside of a catalytic RNA molecule. *Science*, **245**, 276–282.
10. Celander,D.W. and Cech,T.R. (1990) Iron(II)-ethylenediaminetetraacetic acid catalyzed cleavage of RNA and DNA oligonucleotides: similar reactivity toward single- and double-stranded forms. *Biochemistry*, **29**, 1355–1361.

11. Franchet-Beuzit,J., Spotheim-Maurizot,M., Sabattier,R., Blazy-Baudras,B. and Charlier,M. (1993) Radiolytic footprinting. Beta rays, gamma photons and fast neutrons probe DNA-protein interactions. *Biochemistry*, **32**, 2104–2110.
12. Isabelle,V., Franchet-Beuzit,J., Sabattier,R., Spotheim-Maurizot,M. and Charlier,M. (1994) Sites of strand breakage in DNA irradiated by fast neutrons. *Biochimie*, **76**, 187–191.
13. Sclavi,B., Woodson,S., Sullivan,M., Chance,M.R. and Brenowitz,M. (1997) Time-resolved synchrotron X-ray 'footprinting', a new approach to the study of nucleic acid structure and function: application to protein-DNA interactions and RNA folding. *J. Mol. Biol.*, **266**, 144–159.
14. Klassen,N.V. (1987) *Radiation Chemistry Principles and Applications*. Wiley-VCH, New York, pp. 29–61.
15. von Sonntag,C. (1991) The chemistry of free-radical-mediated DNA damage. *Basic Life Sci.*, **58**, 287–321.
16. Hayes,J.J., Kam,L. and Tullius,T.D. (1990) Footprinting protein-DNA complexes with gamma-rays. *Methods Enzymol.*, **186**, 545–549.
17. Sclavi,B., Woodson,S., Sullivan,M., Chance,M. and Brenowitz,M. (1998) Following the folding of RNA with time-resolved synchrotron X-ray footprinting. *Methods Enzymol.*, **295**, 379–402.
18. Hampel,K.J. and Burke,J.M. (2001) Time-resolved hydroxyl-radical footprinting of RNA using Fe(II)-EDTA. *Methods*, **23**, 233–239.
19. Ralston,C.Y., He,Q., Brenowitz,M. and Chance,M.R. (2000) Stability and cooperativity of individual tertiary contacts in RNA revealed through chemical denaturation. *Nat. Struct. Biol.*, **7**, 371–374.
20. Petri,V. and Brenowitz,M. (1997) Quantitative nucleic acids footprinting: thermodynamic and kinetic approaches. *Curr. Opin. Biotechnol.*, **8**, 36–44.
21. Tullius,T.D. and Dombroski,B.A. (1985) Iron(II) EDTA used to measure the helical twist along any DNA molecule. *Science*, **230**, 679–681.
22. Yang,S.W. and Nash,H.A. (1994) Specific photocrosslinking of DNA-protein complexes: identification of contacts between integration host factor and its target DNA. *Proc. Natl Acad. Sci. USA*, **91**, 12183–12187.
23. The EGS4 Code System SLAC. http://www.slac.stanford.edu/cgi-wrap/getdoc/slac-r-265-frontmatter.pdf.
24. Namito,Y., Ban,S. and Hirayama,H. (1995) Compton scattering of 20- to 40-keV photons. *Phys. Rev.*, **51**, 3036–3043.
25. Namito,Y., Ban,S. and Hirayama,H. (1993) Implementation of linearly-polarized photon scattering into the EGS4 code. *Nucl. Instrum. Methods Phys. Res.*, **332**, 277–283.
26. Dixon,W.J., Hayes,J.J., Levin,J.R., Weidner,M.F., Dombroski,B.A. and Tullius,T.D. (1991) Hydroxyl radical footprinting. *Methods Enzymol.*, **208**, 380–413.
27. Birch,R., Marshall,M. and Andran,G.M. (1979) *Catalogue of Spectral Data for Diagnostic X-rays*. Hospital Physicist's Association, London, UK.
28. Tullius,T.D. (1991) DNA footprinting with the hydroxyl radical. *Free Radical Res. Commun.*, **2**, 521–529.
29. Pastor,N., Weinstein,H., Jamison,E. and Brenowitz,M. (2000) A detailed interpretation of OH radical footprints in a TBP-DNA complex reveals the role of dynamics in the mechanism of sequence-specific binding. *J. Mol. Biol.*, **304**, 55–68.
30. Ralston,C.Y., Sclavi,B., Sullivan,M., Deras,M.L., Woodson,S.A., Chance,M.R. and Brenowitz,M. (2000) Time-resolved synchrotron X-ray footprinting and its application to RNA folding. *Methods Enzymol.*, **317**, 353–368.
31. Rice,P.A., Yang,S., Mizuuchi,K. and Nash,H.A. (1996) Crystal structure of an IHF-DNA complex: a protein-induced DNA U-turn. *Cell*, **87**, 1295–1306.
32. Hubell,J.H., Veigele,W.J., Briggs,E.A., Brown,R.T., Cromer,D.T. and Howerton,R.J. (1975) Atomic form factors, incoherent scattering functions and photon scattering cross sections. *J. Phys. Chem. Ref. Data*, **4**, 471.
33. Wu,J.C., Kozarich,J.W. and Stubbe,J. (1983) The mechanism of free base formation from DNA by bleomycin. A proposal based on site specific tritium release from Poly(dA.dU). *J. Biol. Chem.*, **258**, 4694–4697.
34. Heyduk,T., Baichoo,N. and Heyduk,E. (2001) Hydroxyl radical footprinting of proteins using metal ion complexes. *Met. Ions Biol. Syst.*, **38**, 255–287.